Research Square

Preprints are preliminary reports that have not undergone peer review.
They should not be considered conclusive, used to inform clinical practice,
or referenced by the media as validated information.

Synergistic Effect of Akkermansia muciniphila and Bifidobacterium breve on Anti-Tumor Activity Through Targeted Suppression of the COX-2/PGE2 Axis

Yueyue Liu
Zhejiang Provincial People's Hospital
Yanqing Yang
Zhejiang Provincial People's Hospital
Jiaming Yao
Zhejiang Provincial People's Hospital
Wan-Xin Peng
Hangzhou Hospital of Traditional Chinese Medicine
Han Peng
Zhejiang Provincial People's Hospital
Yin-Yuan Mo
moyinyuan@hmc.edu.cn

Zhejiang Provincial People's Hospital

Article

Keywords: Akkermansia muciniphila, Bifidobacterium breve, direct delivery, COX-2, PGE2

Posted Date: November 12th, 2026

DOI: https://doi.org/10.21203/rs.3.rs-10747438/v1

License: This work is licensed under a Creative Commons Attribution 4.0 International License.
Read Full License

Additional Declarations: No competing interests reported.

Synergistic Effect of *Akkermansia muciniphila* and *Bifidobacterium breve* on Anti-Tumor Activity Through Targeted Suppression of the COX-2/PGE2 Axis

Yueyue Liu[1], Yanqing Yang[1], Jiaming Yao[1], Wan-Xin Peng[2], Han Peng[1*], Yin-Yuan Mo[1*]

[1]Center for Translational Medicine, Zhejiang Provincial People's Hospital, (Affiliated People's Hospital), Hangzhou Medical College, Hangzhou, Zhejiang, China.

[2]Department of Surgical Urology, Hangzhou Hospital of Traditional Chinese Medicine, Hangzhou, Zhejiang, China.

[*]Correspondence:

HP, 12107005@zju.edu.cn

Y-Y Mo, moyinyuan@hmc.edu.cn

Key words: *Akkermansia muciniphila*; *Bifidobacterium breve*; direct delivery; COX-2; PGE2;

Abbreviations: AKK, *Akkermansia muciniphila*; Bifido, *Bifidobacterium breve*; IHC,

immunohistochemistry; mIHC, multiplex IHC; PGE2, prostaglandin E2; s.c., subcutaneously; SCFAs, short-chain fatty acids; SPF, specific pathogen-free; TME, tumor microenvironment.

Abstract

The gut microbiome critically modulates anti-tumor immunity, yet whether Akkermansia muciniphila (AKK) and Bifidobacterium breve (Bifido) act synergistically remains unknown. Here, we demonstrate that AKK monotherapy suppresses tumor growth in syngeneic murine colon cancer models while upregulating host Bifido levels. Co-administration of AKK and Bifido produces a reciprocal potentiation of anti-tumor activity exceeding either monotherapy. This combination significantly impairs tumor growth, enhances apoptosis, and increases $CD4^+$ and $CD8^+$ T cell infiltration. Metabolomic profiling revealed that AKK combined with Bifido specifically downregulates prostaglandin E2 (PGE2), which corresponds with marked COX-2 suppression predominantly in tumor cells. Functionally, exogenous PGE2 dose-dependently rescues tumor growth and abolishes the combined therapeutic efficacy. Conversely, COX-2 knockdown or pharmacological inhibition with Celebrex in tumor cells supresses basal tumor growth but neutralizes the additional benefit of combined probiotic therapy, identifying COX-2/PGE2 suppression as an essential mechanism driving this synergistic anti-tumor response. Together, these findings reveal a novelty cross-talk mechanism between Akk and Bifido via suppression of the COX-2/PGE2 axis in tumor cells, establishing a mechanistic rationale for multi-strain probiotic combinations in cancer immunotherapy.

1. Introduction

Cancer remains a leading cause of morbidity and mortality worldwide. Despite remarkable advances in immunotherapy and targeted therapies, response rates remain variable and resistance frequently develops (1,2). In recent years, the gut microbiome has been recognized as a pivotal regulator of anti-tumor immunity and a determinant of therapeutic efficacy (3-7). Seminal studies have demonstrated that specific commensal bacteria, including *Bifidobacterium* species and *Akkermansia muciniphila*, can potentiate responses to immune checkpoint blockade by reshaping the tumor microenvironment and enhancing T cell-mediated immunity (8-11).

Akkermansia muciniphila (AKK), a mucin-degrading bacterium first isolated from the human gastrointestinal tract by Derrien et al. (12), has gained considerable attention for its pleiotropic effects on host metabolic health and barrier integrity (13-17). Its abundance has been positively correlated with favorable clinical responses to PD-1/PD-L1 blockade in patients with non-small cell lung cancer, urothelial carcinoma, and renal cell carcinoma (8,18). *Bifidobacterium breve* (Bifido), a well-established probiotic, has been shown to promote dendritic cell activation(19), resistance to cancer immunotherapy enhance $CD8^+$ T cell priming, and synergize with anti-PD-L1 therapy in preclinical models (9,20). However, most studies have focused on individual probiotic strains, and the potential for synergistic interactions between distinct bacterial species in the context of anti-tumor activity remains

largely unexplored.

The cyclooxygenase-2 (COX-2)/prostaglandin E2 (PGE2) signaling axis is one of the most well-characterized oncogenic pathways in solid tumors (21,22). COX-2, encoded by the *PTGS2* gene, is frequently overexpressed in colorectal and other epithelial cancers and catalyzes the conversion of arachidonic acid to PGE2 (23). PGE2 promotes tumorigenesis through multiple mechanisms, including stimulation of tumor cell proliferation, angiogenesis, and immune evasion by suppressing anti-tumor T cell responses and promoting regulatory T cell and myeloid-derived suppressor cell accumulation (24,25). Pharmacological inhibition of COX-2 with selective inhibitors such as celecoxib has demonstrated anti-tumor activity in preclinical and clinical settings (26). However, whether the gut microbiome can modulate the COX-2/PGE2 axis within the tumor microenvironment has not been systematically investigated.

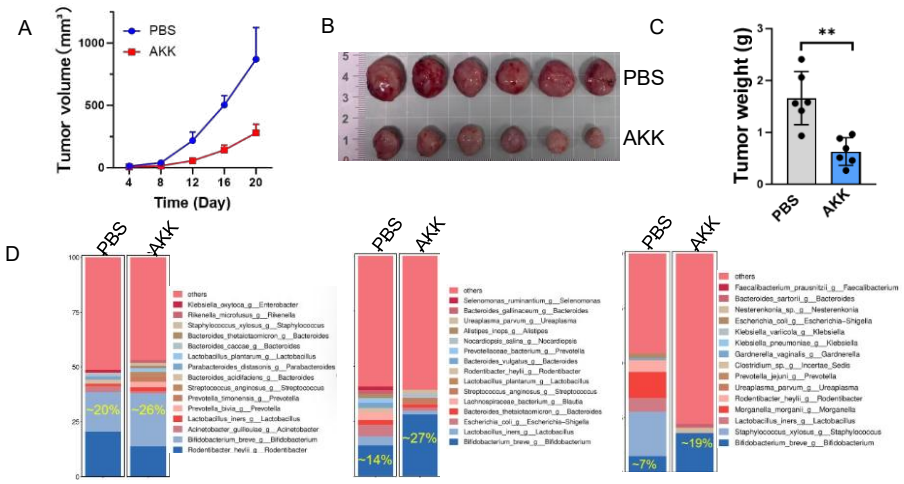
In the present study, we hypothesized that co-administration of AKK and Bifido may produce synergistic anti-tumor effects that exceed those of either probiotic alone, and that this synergy may operate through modulation of tumor-intrinsic metabolic pathways. Using two syngeneic murine colon cancer models, untargeted metabolomics, and genetic and pharmacological perturbation strategies, we demonstrate that AKK and Bifido reciprocally enhance each other's anti-tumor activity through specific suppression of the COX-2/PGE2 axis within tumor cells.

Results

AKK Monotherapy Restrains Tumor Growth and Enriches Intestinal *Bifidobacterium breve*

Our previous study showed that direct mixing of AKK with tumor cells, followed by subcutaneous injection, caused a greater tumor suppression than oral gavage. In this study, we mixed AKK with tumor cells at ratio 1:1, and delivered to C57BL/6 mice through subcutaneous injection. Longitudinal tumor growth curves and endpoint tumor weight quantification showed that AKK significantly slowed MC38 tumor expansion relative to PBS control (Figure 1A~C). Interestingly, 16S rRNA tumor microbiome profiling at study endpoint revealed robust shifts in commensal composition in AKK-treated tumors. For example, the relative abundance of *Bifidobacterium breve* was elevated (~27%) compared with PBS controls (~19%), while pro-inflammatory pathobionts including *Klebsiella pneumoniae* and *Rodentibacter heylii* were depleted (Figure 1D). This positive correlation between AKK administration and enrichment of *B. breve* prompted us to test combinatorial AKK+Bifido intervention for potential synergistic tumor suppression.

Fig.1



127

128 **AKK and Bifido Synergistically Suppress Tumorigenesis in Two Murine Colon**

129 **Cancer Models**

130 To evaluate combinatorial efficacy, four treatment arms were established in both

131 MC38/C57BL/6 and CT26/BALB/c models, PBS, AKK alone, Bifido alone, AKK+Bifido

132 co-administration (Figure 2). Since AKK substantially suppressed tumor growth at 1:1

133 ratio (Figure 1A~C), we intentionally reduced ratio at 1:0.25 (tumor cell:AKK or Bifido)

134 for monotherapy, whereas as for combinatorial therapy, we used 1:0.125+0.125 such

135 that the total amount AKK+Bifido still remained at 1:0.25. In the MC38/C57BL/6 model,

136 AKK or Bifido single-strain treatment induced modest but significant MC38 tumor

137 growth inhibition versus PBS vehicle. By contrast, co-administration of AKK+Bifido

138 produced greater tumor suppression than either agent alone, reflected in reduced

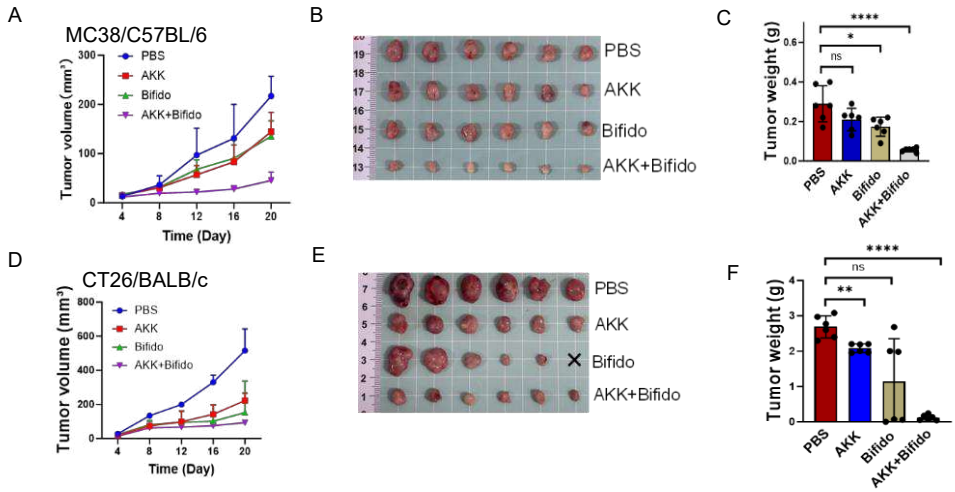
139 tumor volume over the 20-day monitoring window (Figure 2A) and significantly lower

140 endpoint tumor burdens (Figure 2B~C). In the CT26/BALB/c model, we observed a

141 similar pattern (Figure 2D~F). The magnitude of tumor reduction exceeded additive

effects, confirming reciprocal synergism: AKK amplified Bifido-mediated tumor suppression, and Bifido reciprocally enhanced AKK's anti-tumor function across genetically distinct CRC cell lines and host immune backgrounds.

Fig.2



AKK+Bifido Treatment Represses Tumor Proliferation, Induces Apoptosis, and Enhances Intratumoral Anti-Tumor T Cell Infiltration

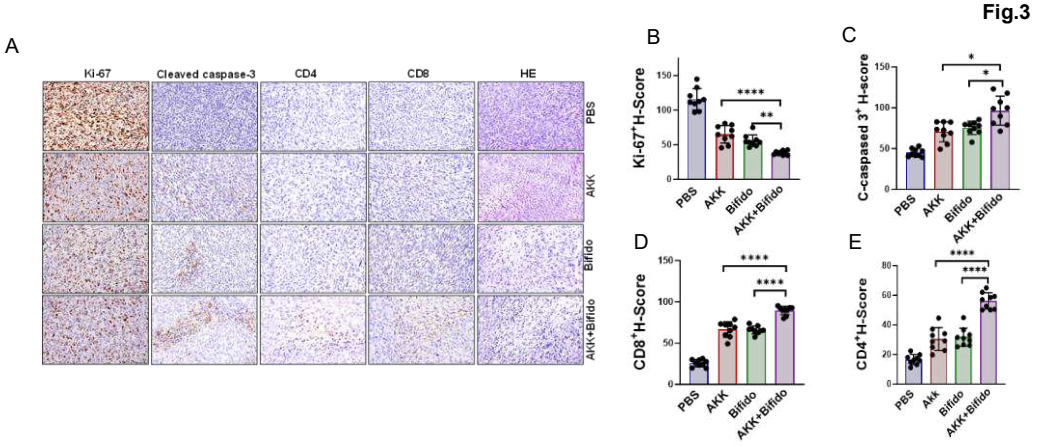
To evaluate the impact of AKK, Bifido, or their combination on tumor morphology and the immune microenvironment, hematoxylin and eosin (H&E) staining was performed on subcutaneous MC38 tumors from each treatment group to characterize cellular and immunological remodeling within the TME (Figure 3A). The PBS control group displayed densely packed tumor cells with abundant eosinophilic cytoplasm, prominent nucleoli, and minimal stromal infiltration, characteristic of highly proliferative, poorly immunogenic tumors. In contrast, tumors from mice treated with AKK alone exhibited subtle morphological changes, with slightly looser cell packing but no overt signs of

necrosis or immune infiltration. Bifido treatment resulted in similar histological alterations, including reduced cellular density, increased intercellular spacing, and focal areas of cellular debris, suggestive of ongoing apoptosis. The most pronounced changes were observed in the AKK+Bifido combination group, where tumors appeared strikingly disorganized and "spongy," with large acellular gaps and extensive infiltration of small, round immune cells into the tumor stroma.

These histopathological observations are consistent with the quantitative findings from Ki-67, cleaved caspase-3, CD8, and CD4 staining (Figure 3B~E). For example, we found the reduction in Ki-67 positivity in the combination group (Figure 3B), while the robust increase in cleaved caspase-3 signals confirms enhanced apoptotic activity (Figure 3C). Furthermore, the elevated $CD8^+$ and $CD4^+$ T cell densities within the tumor parenchyma correlated directly with the loosened stromal architecture seen in H&E sections (Figure 3D~E), suggesting that immune cell recruitment is a major contributor to the structural disintegration of the tumor.

Collectively, these data demonstrate that combined administration of AKK and Bifido synergistically remodels the tumor microenvironment by simultaneously inducing tumor cell apoptosis and promoting intratumoral T lymphocyte infiltration, leading to a profound loss of tumor integrity.

Fig.3



177

178

179 **PGE_2 as a Potential Target of AKK+Bifido Combination Therapy**

180 To determine whether the metabolic reprogramming is involved in the synergistic anti-
181 tumor effects of AKK and Bifido, we performed untargeted metabolomics profiling on
182 tumor tissues from mice treated with PBS, AKK, Bifido, or their combination. As shown
183 in Figure 4A, partial least squares discriminant analysis (PLS-DA) revealed distinct
184 metabolic clustering among all four groups, indicating that each probiotic intervention
185 induced a unique metabolic signature. Notably, the AKK+Bifido combination produced
186 a metabolic profile that was nearly inverse to that of the PBS control across multiple
187 key metabolites (Figure 4B~C), suggesting a profound systemic remodeling of the
188 tumor metabolome.

189

190 Among the differentially regulated metabolites, prostaglandin E_2 (PGE_2) emerged as a
191 particularly compelling candidate. PGE_2 is a well-established immunosuppressive lipid

mediator known to promote tumor progression by inhibiting dendritic cell function, suppressing $CD8^+$ T cell activity, and recruiting regulatory T cells. The COX-2 / PGE2 can cause inflammation and tumorigenesis in colorectal cancer and serve as a key driver of cancer progression (27). In this regard, PGE_2 levels were significantly downregulated in the AKK+Bifido group compared to the PBS control, whereas single-agent treatments showed only modest reductions (Figure 4D).

To validate this finding at the protein level, we performed immunohistochemistry (IHC) staining for cyclooxygenase-2 (COX-2), the rate-limiting enzyme responsible for PGE_2 biosynthesis. Consistent with the metabolomics data, COX-2 expression was markedly reduced in the AKK+Bifido group relative to controls (Fig. 4E~F).

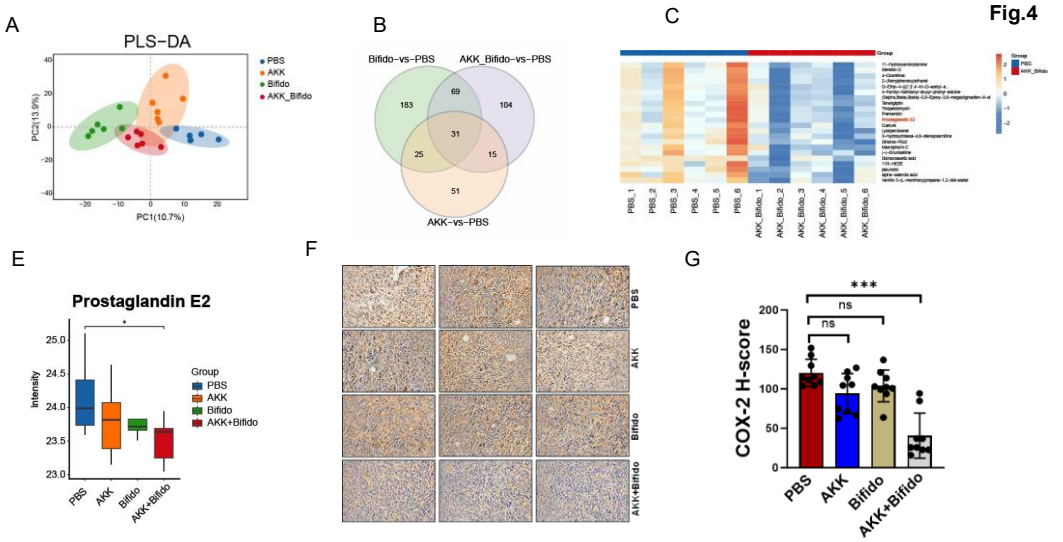


Fig.4

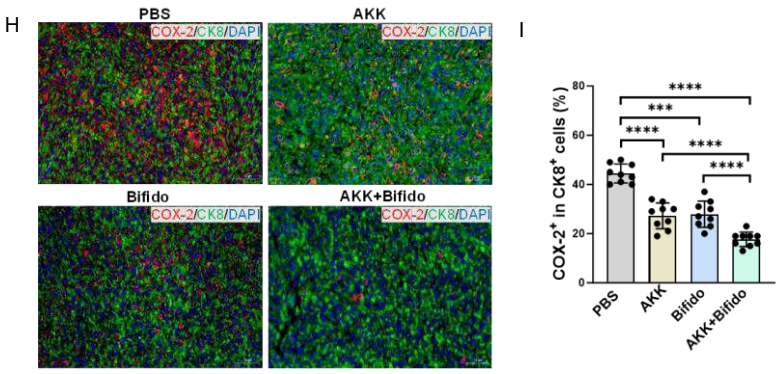
AKK+Bifido Downregulates COX-2 Expression Predominantly in Tumor Cells

To determine the cellular source of COX-2 downregulation, we performed multiplex IHC (mIHC) co-staining for COX-2 and cytokeratin 8 (CK8, a tumor cell marker). This analysis

confirmed that COX-2 downregulation occurred predominantly within $CK8^+$ tumor cells rather than in stromal or immune cell compartments (Fig. 4H~I). The percentage of $COX\text{-}2^+/CK8^+$ double-positive cells was significantly reduced in the AKK+Bifido group compared to all other treatment groups.

Taken together, these results identify PGE_2 as a key metabolic node through which AKK+Bifido combination therapy may exert its anti-tumor effects. The coordinated downregulation of PGE_2 and its biosynthetic enzyme COX-2 provides a mechanistic link between probiotic-induced metabolic reprogramming and the enhanced $CD4^+/CD8^+$ T cell infiltration observed in our earlier histological analyses.

Fig.4



Exogenous PGE_2 Rescues Tumor Growth Suppression by AKK+Bifido

To functionally validate PGE_2 as a downstream mediator of AKK+Bifido activity, we performed exogenous PGE_2 dose-rescue experiments in MC38 tumor-bearing mice receiving AKK+Bifido (Figure 5). Compared with AKK+Bifido + DMSO vehicle control,

incremental supplementation of 20 μg, 40 μg, and 60 μg PGE_2 dose-dependently reversed tumor growth inhibition, with the highest PGE_2 dose fully ablating the combinatorial anti-tumor phenotype (Figure 5A~C).

Pharmacological COX-2 Inhibition Phenocopies the Anti-Tumor Effect of AKK+Bifido

To further corroborate the role of the COX-2/PGE2 axis, we treated tumor-bearing mice with Celebrex, a selective COX-2 inhibitor. Celebrex monotherapy significantly reduced tumor volume and weight relative to vehicle control, recapitulating the core anti-tumor phenotype of AKK+Bifido co-treatment (Figure 5D~F). When Celebrex was combined with AKK+Bifido, no further additive tumor suppression was observed, indicating probiotics and Celebrex converge on the identical COX-2/PGE_2 effector pathway.

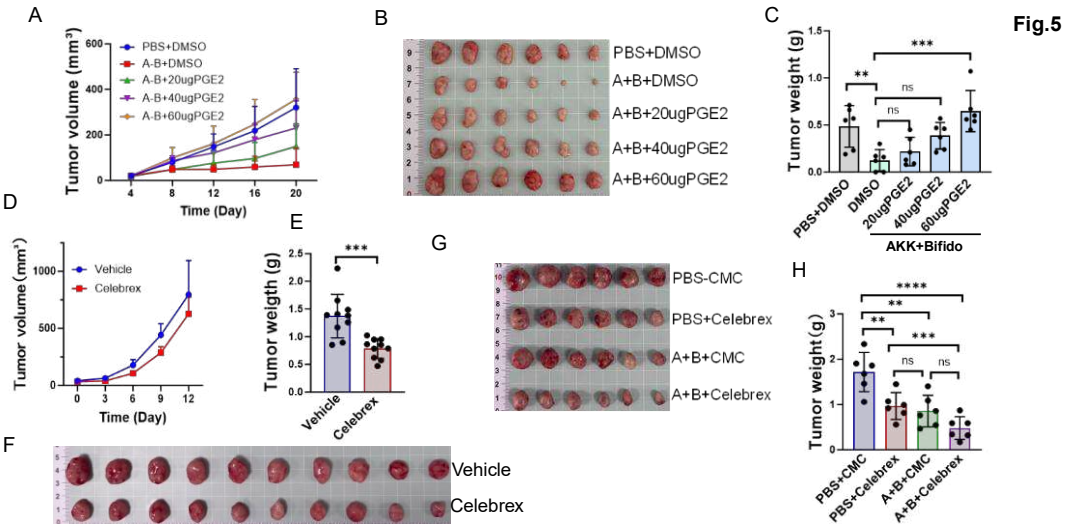


Fig.5

COX-2 Overexpression Promotes, While COX-2 Knockdown Suppresses, Tumor

Growth Mediated by AKK or Bifido

To delineate the functional role of COX-2 in mediating the anti-tumor effects of AKK and Bifido, we utilized CT26 murine colon carcinoma cells engineered to overexpress COX-2 (as a COX-2-mCherry fusion protein, Figure 6A) or silence COX-2 via shRNA-mediated knockdown (Figure 6E). We then assessed tumor growth in these genetic backgrounds with or without probiotic treatment.

Tumor growth kinetics (Figure 6B) and final tumor burdens (Figure 6C~D) revealed that COX-2 overexpression significantly enhanced tumor growth, even in the presence of AKK or Bifido. Specifically, Vector-PBS tumors grew rapidly, while Vector-AKK, Vector-Bifido, and Vector-AKK+Bifido showed marginal growth inhibition. In contrast, OE-COX-2 tumors (regardless of probiotic co-treatment) exhibited accelerated growth, with OE-PBS, OE-AKK, OE-Bifido, and OE-AKK+Bifido all displaying larger tumor volumes and weights than their vector counterparts. Statistical analysis (Fig. 6D) confirmed that COX-2 overexpression abrogated the modest anti-tumor effects of AKK or Bifido.

COX-2 knockdown model (Figure 6E) revealed that tumor growth curves (Figure 6F) and tumor burdens (Figure 6G~H) were suppressed by shRNA across all probiotic conditions. Notably, shRNA-PBS tumors showed baseline growth, while shRNA-AKK, shRNA-Bifido, and shRNA-AKK+Bifido exhibited significantly reduced tumor burdens. The combination of COX-2 knockdown with AKK+Bifido (shRNA-AKK+Bifido) yielded

the most dramatic suppression of tumor growth, with tumor volumes and weights lower than any other group.

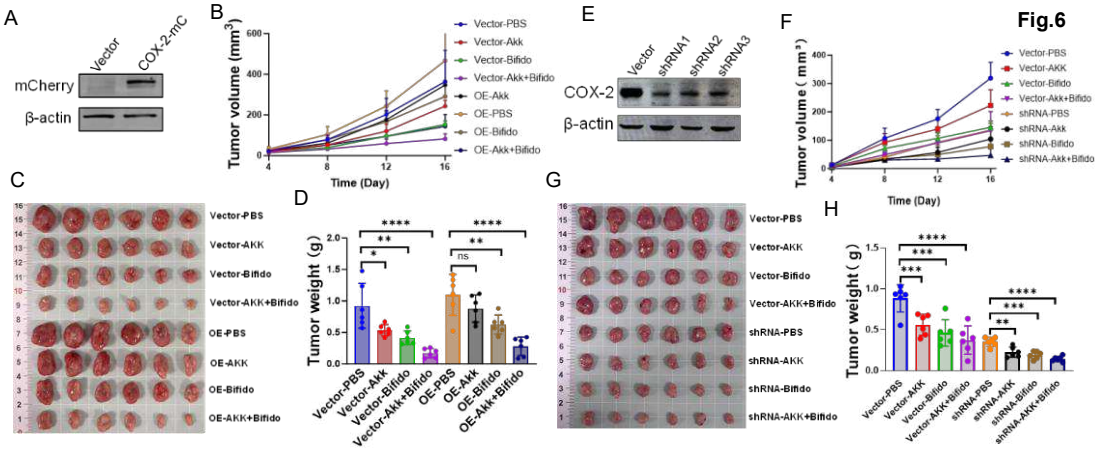


Fig.6

Collectively, these gain- and loss-of-function experiments in CT26 cells establish that COX-2 is a critical downstream mediator of AKK- and Bifido-induced tumor growth regulation. Overexpressing COX-2 overrides the protective effects of probiotics, whereas silencing COX-2 enhances their anti-tumor efficacy. These findings support a model in which AKK and Bifido suppress tumor growth, at least in part, by inhibiting the COX-2 axis, either by reducing COX-2 expression (as seen with shRNA) or by counteracting its pro-tumorigenic activity (as seen with overexpression).

Discussion

In this study, we demonstrate that the probiotics *Akkermansia muciniphila* and *Bifidobacterium breve* act synergistically to suppress tumor growth in murine colon cancer

models through specific targeting of the COX-2/PGE2 axis within tumor cells. Our findings reveal a previously unrecognized mechanism by which defined gut microbial communities can reprogram tumor-intrinsic metabolic pathways to promote anti-tumor immunity.

The observation that AKK monotherapy was associated with endogenous expansion of *Bifidobacterium breve* (Fig. 1D) is consistent with the concept of microbial cross-feeding and ecological succession within the gut microbiome (28). AKK-mediated degradation of mucin glycoproteins generates short-chain fatty acids and oligosaccharides that may serve as substrates for bifidobacterial growth (13,29). This ecological interaction may explain, at least in part, the synergistic anti-tumor effects observed with co-administration: AKK may create a favorable tumor microenvironment niche that supports Bifido colonization, thereby amplifying the collective immunomodulatory output.

The identification of PGE2 as the key metabolite differentially regulated by AKK+Bifido (Fig. 4D) provides a mechanistic link between probiotic treatment and tumor suppression. PGE2 is a well-established mediator of tumor immune evasion, functioning through EP receptor signaling to suppress dendritic cell maturation, inhibit natural killer cell cytotoxicity, promote regulatory T cell differentiation, and drive myeloid-derived suppressor cell expansion (10,24,25,30). The demonstration that exogenous PGE2 administration dose-dependently reversed the synergistic anti-tumor effect (Fig. 5A) provides strong causal evidence that PGE2 suppression is necessary for the observed tumor inhibition, suggesting that mechanistic link between microbial metabolites and tissue-level gene expression (31). Our results further support that PGE2 is a potential therapeutic target (32) which may achieve

by utilization of probiotics in this case. Future studies will determine whether pharmacological inhibition of the COX-2/PGE_2 pathway can recapitulate the therapeutic benefits of AKK+Bifido treatment.

Our finding that COX-2 downregulation occurs predominantly within $CK8^+$ tumor cells (Fig. 4H-I) is particularly noteworthy, as it suggests that AKK+Bifido can modulate tumor-intrinsic gene expression programs, potentially through microbiome-derived metabolites or immune-mediated paracrine signaling that reaches the tumor. This is consistent with emerging evidence that microbial metabolites, including short-chain fatty acids, secondary bile acids, and tryptophan catabolites, can systemically circulate and influence distal tissue gene expression (33,34). Future studies should investigate the specific microbial metabolites or immune mediators that link tumor colonization by AKK and Bifido to intratumoral COX-2 suppression.

The genetic validation using COX-2 shRNA knockdown (Fig. 6) provides further evidence that COX-2 expression in tumor cells is a prerequisite for the synergistic anti-tumor activity of AKK+Bifido. In the absence of tumor cell COX-2, the probiotic combination conferred no additional benefit over PBS treatment, indicating that the synergy operates specifically through this pathway rather than through parallel, COX-2-independent mechanisms. This finding has important clinical implications, as it suggests that the efficacy of probiotic-based interventions may be context-dependent and influenced by the COX-2 expression status

of the tumor.

The concordance between pharmacological COX-2 inhibition with Cerebrex and probiotic-mediated COX-2 suppression (Fig. 5) further supports the therapeutic relevance of this pathway. COX-2 inhibitors have demonstrated chemopreventive and therapeutic efficacy in colorectal cancer but are associated with cardiovascular toxicity with prolonged use (20,23,26). Probiotic-mediated COX-2 suppression may represent a safer, complementary approach to modulating this pathway, either as monotherapy or in combination with reduced-dose pharmacological inhibitors.

Our findings also have implications for understanding heterogeneity in clinical responses to probiotic and microbiome-based interventions. The requirement for COX-2 expression in the tumor for the synergistic effect suggests that patient stratification based on tumor COX-2 status may be necessary to identify responders. Moreover, the demonstration that synergistic interactions between distinct bacterial species can produce qualitatively different effects than individual strains underscores the importance of designing rational microbial consortia rather than relying on single-strain interventions (20,35,36).

Several limitations of this study should be acknowledged. First, the use of syngeneic murine models, while informative for mechanistic studies, may not fully recapitulate the complexity of human tumor-microbiome interactions. Second, the precise molecular mediators linking gut colonization by AKK and Bifido to intratumoral COX-2 suppression

remain to be identified. Third, the relative contributions of direct metabolite signaling versus immune-mediated mechanisms require further investigation. Future studies employing germ-free mice, metabolite supplementation, and comprehensive immune profiling will be essential to dissect these mechanisms and to evaluate the translational potential of AKK+Bifido combination therapy in human cancer.

In summary, this study provides the first evidence that *Akkermansia muciniphila* and *Bifidobacterium breve* synergistically suppress colon tumor growth in murine models through specific targeting and downregulation of the COX-2/PGE2 axis in tumor cells. These findings advance our understanding of how defined probiotic consortia can reprogram tumor metabolism and immunity, and they provide a rationale for developing combinatorial probiotic strategies as adjunctive cancer therapies.

Materials and Methods

Cell culture

Murine colorectal cancer cell lines MC38 and CT26 were obtained from the Cell Bank of the Chinese Academy of Sciences (Shanghai). Cells were maintained in Dulbecco's Modified Eagle Medium (DMEM) supplemented with 10% fetal bovine serum and 1% penicillin–streptomycin, and incubated at 37°C in a humidified atmosphere containing 5% CO2. All cell lines were confirmed to be mycoplasma-free by PCR prior to use.

Animals

The animal use protocol listed below has been reviewed and approved by the Institution Animal Care and Use Committee(IACUC),ZJCLA

Specific pathogen-free (SPF) female C57BL/6 and BALB/c mice (4–6 weeks old) were purchased from Hangzhou Medical College Animal Center and acclimated for one week before experimental procedures. Animals were housed under SPF conditions at 22–23°C with a 12 h light/12 h dark cycle and ad libitum access to food and water. All procedures were approved by the Institutional Animal Care and Use Committee，Zhejiang Center of Laboratory Animals, Hangzhou Medical College (ZJCLA-IACUC-20010660 and ZJCLA-IACUC-20060072), Confirming that all experiments were performed in accordance with relevant guidelines and regulations.

At the experimental endpoint, mice were humanely euthanized via deep inhalation anesthesia with 5% isoflurane (R510-22-10, RWD, China) in an induction chamber (approximately 4 L/min O_2 flow) until respiratory arrest, followed by cervical dislocation to ensure death.

Culture of *Akkermansia muciniphila* and *Bifidobacterium breve*

Akkermansia muciniphila (AKK, ATCC BAA-835) and *Bifidobacterium breve* (Bifido) were obtained from Biobw Biotech Co., Ltd. (Beijing, China). AKK was cultured under a gas mixture of 90% N2, 5% H2, and 5% CO2 in brain heart infusion (BHI) medium supplemented with mucin and Bifido was cultured anaerobically in MRS medium.

Colony-forming units per milliliter (CFU/mL) were determined by plating representative stocks on agar medium. For in vivo use, cultures were harvested by centrifugation, washed twice with PBS, and finally resuspended in PBS.

Delivery of AKK to animals

AKK was prepared as above and mixed with tumor cells at an appropriate ratio as indicated. For example, for 1:1 ratio (bacterium:tumor cell) we used 1×10^6 CFU AKK and 1×10^6 tumor cells, and 100 μL of the mixture was injected s.c. For combined treatment, we used 0.25 (0.125+0.125 for combination):1 ratio. Tumor growth was monitored and measured by caliper every four days. Tumor volume (mm^3) was calculated as $d^2 \times D / 2$, where d and D are the shortest and longest tumor diameters (mm), respectively.

H&E staining

For hematoxylin and eosin (H&E) staining, tumor tissues were fixed in 4% paraformaldehyde (P1110, Solarbio) immediately after tumors were harvested. The fixed tissues were dehydrated in ethanol, cleared in xylene, and then embedded in paraffin. The processed tissues were sectioned and stained H&E with solution. Images were captured using APX100 microscope.

Immunohistochemistry (IHC)

For immunohistochemical (IHC) staining, tissue sections were deparaffinized and rehydrated, followed by incubation with an endogenous peroxidase blocker (HK10020A, Hao Ke). Antigen retrieval was performed, and the sections were subsequently blocked with 5% bovine serum albumin (BSA). The tissue slides were then incubated overnight at 4°C with primary antibodies against Ki-67 (CY5542, Abways; 1:200), CD4 (25229S, CST; 1:100), CD8-alpha (98941S, CST; 1:400), and cleaved caspase-3 (98941S, CST; 1:400). Thereafter, the slides were incubated with a secondary antibody (HK10020B, Hao Ke) for 1 hour at room temperature. Signal visualization was achieved using a DAB substrate solution, resulting in brown staining. The slides were then counterstained with hematoxylin. Quantitative analysis was performed based on both staining intensity and the proportion of positive cells using the H-score method (37).

Immunohistofluorescence

For the immunohistofluorescence procedure, paraffin-embedded tissue sections were deparaffinized and rehydrated, followed by antigen retrieval and quenching of endogenous peroxidase activity as described above. Next, the sections were incubated with the primary antibody overnight at 4°C. After washing, the tissue sections were completely covered with Poly-HRP Goat Anti-Rabbit Secondary Antibody (H+L) (HKI0026) and incubated at room temperature for 50 minutes in the dark. Tyramide signal amplification (TSA) was performed using Flare570 Super-Sensitive Concentrate (red; HKI0015S) for COX-2 detection and Flare520 Super-Sensitive Concentrate (green; HKI0014S) for CK8 detection. An additional antigen retrieval step was

performed between the two rounds of staining to remove residual antibodies. Finally, nuclei were counterstained with DAPI, and the sections were mounted with an anti-fade mounting medium prior to imaging.

Quantification of immunohistofluorescence for $CK8^{+}Cox\text{-}2^{+}$ cell populations

To perform automated cell-level quantification of fluorescence-labeled markers across selected images (predominantly from the peritumoral region), we employed QuPath v4.3 integrated with the OpenSlide library for robust image loading and channel separation. Specific parameters were set to automatically detect and annotate the entire selected area.

For the immunofluorescence quantification phase, we utilized the built-in IF analysis module to define per-channel detection thresholds and intensities, enabling precise identification of positive cells within each channel. To ensure data integrity, a thorough quality control review of the detections was conducted before exporting the validated metrics, cell counts, and representative annotations for downstream analysis.

Construction of plasmids

For overexpression, the mouse PTGS2 coding region was initially amplified from cDNA of MC38 cells using the primers and Phusion enzyme (NEB), and then cloned into a pCDH lentivirus vector (System Bioscience). To better monitor its expression, we introduced mCherry to make mCherry-PTSE2 fusion. Cloning procedure used

seamless cloning kit provided by the manufacturer (Abclonal).

mC-PTGS2-Xho1-5.1, CCGGACTCAGATGGCTCGAGCTCTTCCGAGCTGTGCTGCT

PTGS2-mC-BamH1-3.1, TATCTAGATCCGGTGGATCCTCACTTGTCATCGTCGTCCTTGTAGTC

PTGS2 shRNA was cloned into pLKO.1-Puro with following sequences:

PTGS2-shRNA1, GCTGACATCCAGATCATATTT;

PTGS2-shRNA2, CATGGGTGTGAAGGGAAATAA;

PTGS2-shRNA3, GGCCATGGAGTGGACTTAAAT.

All cloned sequences were verified by Sanger sequencing method.

Western blot

Total protein extraction and concentration determination were performed following a previously published protocol (38). Briefly, cell pellets were lysed in RIPA lysis buffer supplemented with a protease inhibitor cocktail, subjected to 60 s of sonication, and then rotated continuously at 4°C for 30 min. Lysates were centrifuged at 15,000 × g for 20 min; the resulting supernatants were collected into new tubes and mixed with 5× SDS protein loading buffer to a 1× working concentration. After heating at 95°C for 10 min, protein samples were separated via SDS-PAGE and electrotransferred onto PVDF membranes. Membranes were sequentially probed with primary antibodies and fluorophore-conjugated secondary antibodies labeled with IRDye 800CW or IRDye 680. Immunoblot signals were visualized using the Odyssey Infrared Imaging System (LI-COR Biosciences).

Lentivirus infection

Lentivirus was packaged in 293T cells using the third generation of packaging system, and the virus containing culture medium was collected 48 hours after transfection and filtrated with a filter (4.5 μm). Lentivirus infection was carried out in six-well plates by mixing 500 μL virus supernatant + 500 μL medium containing 8 μg polybrene.

Statistical analysis

The experiments were replicated at least three times. Differences between two experimental groups were analyzed by the unpaired two-sided Student's test, whereas comparisons among three or more groups were made by ANOVA followed, if significant, by the Bonferroni post hoc test. All mathematical analyses of the data were performed using GraphPad Prism 10, and $p < 0.05$ was considered significant.

Data availability statement

The datasets generated and/or analysed during the current study are available in the [OMIX] repository, [https://ngdc.cncb.ac.cn/omix/preview/gQWbn2GB, OMIX: OMIX018866].

Acknowledgement

The authors have no conflicts of interest to declare. All members of the research team confirm that there are no competing interests in relation to this work.

Funding

This research was supported by grants from Natural Science Foundation of China (No. 32500101).

515

516 **Reference:**

517

518 1. Hanahan D. Hallmarks of Cancer: New Dimensions. Cancer Discov **2022**;12:31-46

519 2. Sharma P, Goswami S, Raychaudhuri D, Siddiqui BA, Singh P, Nagarajan A*, et al.* Immune

520 checkpoint therapy-current perspectives and future directions. Cell **2023**;186:1652-69

521 3. Routy B, Le Chatelier E, Derosa L, Duong CPM, Alou MT, Daillere R*, et al.* Gut microbiome

522 influences efficacy of PD-1-based immunotherapy against epithelial tumors. Science

523 **2018**;359:91-7

524 4. Gopalakrishnan V, Spencer CN, Nezi L, Reuben A, Andrews MC, Karpinets TV*, et al.* Gut

525 microbiome modulates response to anti-PD-1 immunotherapy in melanoma patients.

526 Science **2018**;359:97-103

527 5. Matson V, Fessler J, Bao R, Chongsuwat T, Zha Y, Alegre ML*, et al.* The commensal

528 microbiome is associated with anti-PD-1 efficacy in metastatic melanoma patients.

529 Science **2018**;359:104-8

530 6. Sears CL, Garrett WS. Microbes, microbiota, and colon cancer. Cell Host Microbe

531 **2014**;15:317-28

532 7. Vetizou M, Pitt JM, Daillere R, Lepage P, Waldschmitt N, Flament C*, et al.* Anticancer

533 immunotherapy by CTLA-4 blockade relies on the gut microbiota. Science

534 **2015**;350:1079-84

535 8. Routy B, Gopalakrishnan V, Daillere R, Zitvogel L, Wargo JA, Kroemer G. The gut

536 microbiota influences anticancer immunosurveillance and general health. Nat Rev Clin

Oncol **2018**;15:382-96

9. Sivan A, Corrales L, Hubert N, Williams JB, Aquino-Michaels K, Earley ZM*, et al.* Commensal Bifidobacterium promotes antitumor immunity and facilitates anti-PD-L1 efficacy. Science **2015**;350:1084-9

10. Wang Q, Meng Q, Chen Y, Liu Y, Li X, Zhou J*, et al.* Interaction between gut microbiota and immunity in health and intestinal disease. Front Immunol **2025**;16:1673852

11. Zheng D, Liwinski T, Elinav E. Interaction between microbiota and immunity in health and disease. Cell Res **2020**;30:492-506

12. Derrien M, Vaughan EE, Plugge CM, de Vos WM. Akkermansia muciniphila gen. nov., sp. nov., a human intestinal mucin-degrading bacterium. Int J Syst Evol Microbiol **2004**;54:1469-76

13. Depommier C, Everard A, Druart C, Plovier H, Van Hul M, Vieira-Silva S*, et al.* Supplementation with Akkermansia muciniphila in overweight and obese human volunteers: a proof-of-concept exploratory study. Nat Med **2019**;25:1096-103

14. Plovier H, Everard A, Druart C, Depommier C, Van Hul M, Geurts L*, et al.* A purified membrane protein from Akkermansia muciniphila or the pasteurized bacterium improves metabolism in obese and diabetic mice. Nat Med **2017**;23:107-13

15. Gao F, Cheng C, Li R, Chen Z, Tang K, Du G. The role of Akkermansia muciniphila in maintaining health: a bibliometric study. Front Med (Lausanne) **2025**;12:1484656

16. Belzer C, de Vos WM. Microbes inside--from diversity to function: the case of Akkermansia. ISME J **2012**;6:1449-58

17. van der Lugt B, van Beek AA, Aalvink S, Meijer B, Sovran B, Vermeij WP*, et al.* Akkermansia

559 muciniphila ameliorates the age-related decline in colonic mucus thickness and
560 attenuates immune activation in accelerated aging Ercc1 (-/Delta7) mice. Immun Ageing
561 **2019**;16:6
562 18. Derosa L, Hellmann MD, Spaziano M, Halpenny D, Fidelle M, Rizvi H*, et al.* Negative
563 association of antibiotics on clinical activity of immune checkpoint inhibitors in patients
564 with advanced renal cell and non-small-cell lung cancer. Ann Oncol **2018**;29:1437-44
565 19. Li Q, Li Y, Wang Y, Xu L, Guo Y, Wang Y*, et al.* Oral administration of Bifidobacterium breve
566 promotes antitumor efficacy via dendritic cells-derived interleukin 12. Oncoimmunology
567 **2021**;10:1868122
568 20. O'Callaghan A, van Sinderen D. Bifidobacteria and Their Role as Members of the Human
569 Gut Microbiota. Front Microbiol **2016**;7:925
570 21. Greenhough A, Smartt HJ, Moore AE, Roberts HR, Williams AC, Paraskeva C*, et al.* The
571 COX-2/PGE2 pathway: key roles in the hallmarks of cancer and adaptation to the tumour
572 microenvironment. Carcinogenesis **2009**;30:377-86
573 22. Eberhart CE, Coffey RJ, Radhika A, Giardiello FM, Ferrenbach S, DuBois RN. Up-regulation
574 of cyclooxygenase 2 gene expression in human colorectal adenomas and
575 adenocarcinomas. Gastroenterology **1994**;107:1183-8
576 23. Zelenay S, van der Veen AG, Bottcher JP, Snelgrove KJ, Rogers N, Acton SE*, et al.*
577 Cyclooxygenase-Dependent Tumor Growth through Evasion of Immunity. Cell
578 **2015**;162:1257-70
579 24. Kalinski P. Regulation of immune responses by prostaglandin E2. J Immunol **2012**;188:21-
580 8

25. Nakanishi M, Rosenberg DW. Multifaceted roles of PGE2 in inflammation and cancer. Semin Immunopathol **2013**;35:123-37

26. Patrignani P, Patrono C. Aspirin and Cancer. J Am Coll Cardiol **2016**;68:967-76

27. Wang D, Dubois RN. The role of COX-2 in intestinal inflammation and colorectal cancer. Oncogene **2010**;29:781-8

28. Belkaid Y, Hand TW. Role of the microbiota in immunity and inflammation. Cell **2014**;157:121-41

29. Tanoue T, Morita S, Plichta DR, Skelly AN, Suda W, Sugiura Y*, et al.* A defined commensal consortium elicits CD8 T cells and anti-cancer immunity. Nature **2019**;565:600-5

30. Sinha P, Clements VK, Fulton AM, Ostrand-Rosenberg S. Prostaglandin E2 promotes tumor progression by inducing myeloid-derived suppressor cells. Cancer Res **2007**;67:4507-13

31. Levy M, Thaiss CA, Zeevi D, Dohnalova L, Zilberman-Schapira G, Mahdi JA*, et al.* Microbiota-Modulated Metabolites Shape the Intestinal Microenvironment by Regulating NLRP6 Inflammasome Signaling. Cell **2015**;163:1428-43

32. Fulton AM, Ma X, Kundu N. Targeting prostaglandin E EP receptors to inhibit metastasis. Cancer Res **2006**;66:9794-7

33. Iida N, Dzutsev A, Stewart CA, Smith L, Bouladoux N, Weingarten RA*, et al.* Commensal bacteria control cancer response to therapy by modulating the tumor microenvironment. Science **2013**;342:967-70

34. Viaud S, Saccheri F, Mignot G, Yamazaki T, Daillere R, Hannani D*, et al.* The intestinal microbiota modulates the anticancer immune effects of cyclophosphamide. Science

2013;342:971-6

35. Zitvogel L, Ayyoub M, Routy B, Kroemer G. Microbiome and Anticancer Immunosurveillance. Cell **2016**;165:276-87

36. Helmink BA, Khan MAW, Hermann A, Gopalakrishnan V, Wargo JA. The microbiome, cancer, and cancer therapy. Nat Med **2019**;25:377-88

37. Awad MM, Oxnard GR, Jackman DM, Savukoski DO, Hall D, Shivdasani P*, et al.* MET Exon 14 Mutations in Non-Small-Cell Lung Cancer Are Associated With Advanced Age and Stage-Dependent MET Genomic Amplification and c-Met Overexpression. J Clin Oncol **2016**;34:721-30

38. Peng WX, Liu F, Jiang JH, Yuan H, Zhang Z, Yang L*, et al.* N6-methyladenosine modified LINC00901 promotes pancreatic cancer progression through IGF2BP2/MYC axis. Genes Dis **2023**;10:554-67

Figure legend

Figure1 AKK suppresses tumor growth and is associated with upregulation of Bifidobacterium breve (Bifido). A, Tumor (MC38) growth curve when treated with AKK or PBS, B, Image of tumors, C, Average tumor weights. D, Treatment with AKK is associated with upregulation of Bifido.

Figure 2 AKK synergistically suppress tumorigenesis with Bifidobacterium breve (Bifido). A~C, MC38/C57BL/6 model. Tumor growth curve when treated with AKK or Bifido or AKK+Bifido or PBS (A), image of tumors (B) and average tumor weights (C). D~F, CT26/BALB/c model. Tumor growth curve when treated with AKK or Bifido or AKK+Bifido or PBS (D), image of tumors (E) and average tumor weights (F). “X”, no tumor formed.

Figure 3 AKK+Bifido co-administration suppresses cell proliferation and increases cleaved caspase 3, CD4 and CD8 signals. A, IHC staining of tumor treated with PBS, AKK, Bifido and AKK+Bifido, respectively. B, H-Score for Ki-67. C, H-Score for cleaved caspase 3 signals. D, H-Score for CD8 signals. E, H-Score for CD4 signals.

Figure 4 Metabolomics analysis reveals that PGE2 is a potential target for AKK+Bifido. A, treatment with AKK, Bifido or a combination of both significantly alters the metabolic profile of the subjects compared to the PBS control, with each treatment producing a distinguishable signature. B&C, AKK+Bifido treatment creates a metabolic signature that

is almost the opposite of the PBS control for many key metabolites. D, PGE2 is significantly downregulated as compared to PBS control. E&F, IHC staining reveals that COX-2 is also downregulated by AKK+Bifido. H&I, mIHC staining indicates that tumor cell COX-2 is downregulated by AKK+Bifido.

Figure 5 PGE2 impacts tumor growth. A, PGE2 can neutralizes the tumor suppression action by AKK+Bifido, as shown by tumor growth curve. B, Tumor image and C, Average tumor weight. D~F, Celebrex can suppress tumor growth. G&H, AKK+Bifido further enhance the tumor suppression by Celebrex.

Figure 6 Overexpression of COX-2 increases whereas COX-2 shRNA (shRNA #2) suppresses tumor growth mediated by AKK or Bifido or both. A, Detection of overexpression of COX-2 as COX-2-mCherry fusion protein in CT26 cells by Western blot. B~D, Overexpression of COX-2 increases tumor growth. E, Knockdown of COX-2 in CT26 as determined by Western blot. F~H, Knockdown of COX-2 leads to suppression of tumor growth.

Supplementary Files

This is a list of supplementary files associated with this preprint. Click to download.

- WB.pdf